HEFAT2012
9th International Conference on Heat Transfer, Fluid Mechanics and Thermodynamics
16 – 18 July 2012
Malta

WAKE CONTROL USING SYNTHETIC JETS

BenChiekh M.*, Ferchichi M.** and Béra J. C. ***
* LESTE, Ecole Nationale d'Ingénieurs de Monastir,
Universty of Monastir
5019, Monastir,
Tunisia,
E-mail: maher.benchiekh@enim.rnu.tn
** Royal Military College of Canada, PO Box 17000, Kingston, Ontario, Canada
*** Université Lyon1, Lyon, France ; U1032, France

ABSTRACT

The interactions of wake of an elongated bluff body and the periodic flow emanating from a pair of synthetic jets placed symmetrically at the trailing edge, spanning the width of the plate, were experimentally studied for the purpose of quantifying the flow physics that led to wake drag reduction. The experiments were carried out in a low turbulence wind tunnel at Reynolds number, Re_h based on the flat plate thickness h, of about 7200. The synthetic jet actuators, providing a global momentum addition of Cμ=24%, were positioned symmetrically at the model base at a distance of ± 0.27 h from the base centerline to introduce perturbations at early stages of the shear layers' development. The synthetic jet actuation frequency was selected to be about 75% the vortex shedding frequency of the natural wake. Two-component velocity measurements were acquired using Particle Image Velocimetry (PIV) and reported for natural wake and controlled wake using symmetric synchronous actuation and out-of-phase actuation. In this work, mean velocity profiles, Reynolds stresses and coherent structures and their dynamics in the wake of a bluff body were evaluated as the initial conditions (injection configurations) were changed. Furthermore, phase-averaged velocity fields through the vorticity contours were determined to provide insights into the actuation mechanisms namely, the role of the synthetic jet vortex structures on the flow dynamics.

INTRODUCTION

Flows over bluff bodies have been greatly investigated in the literature due to their fundamental importance in understanding shear layer roll-up, and the subsequent formation of the Bernard-Karman vortex shedding in the wake. Bluff body flows are dominated by high frequency convective instabilities dominating the separating shear layer and lower frequency absolute instabilities governing the vortex shedding in the near wake [1]. These instabilities make bluff body flows very attractive benchmark setup for flow control studies namely, to develop control strategies for the suppression of the vortex shedding which has been strongly affects the pressure dag on blunt objects and results in periodically oscillating aerodynamic forces. Various passive and active control techniques have been developed and studied experimentally and numerically to increase the base pressure by suppression of the vortex shedding so that the rolling up of the separating shear layers starts farther downstream, or by the decoupling of the lower and upper shear layers so that less energy is dissipated. A comprehensive account of these studies can be found in Gad-el-Hak [2] and Choi et al [3].

NOMENCLATURE

C_D		Drag coefficient
$C_{D,mean}$		Drag component resulting from mean momentum transfer
$C_{D,turb}$		Drag component resulting from fluctuating momentum transfer
C_μ		Momentum addition coefficient
c	[m]	Chord length of the model
e	[m]	Width slot
f_o	[Hz]	Vortex shedding frequency
f_A	[Hz]	Actuation frequency
h	[m]	Height length of the model
l_b	[m]	Recirculation bubble length
u	[m.s^{-1}]	Fluctuating component of streamwise velocity
U	[m.s^{-1}]	Mean value of streamwise velocity
$u_{A,max}$	[m.s^{-1}]	Maximum actuation velocity at slot exit
U_∞	[m.s^{-1}]	Free-stream velocity
V	[m.s^{-1}]	Mean value of transverse velocity
v	[m.s^{-1}]	Fluctuating component of transverse velocity
w	[m]	spanwise width of the model
x	[m]	Cartesian axis direction
y	[m]	Cartesian axis direction
z	[m]	Cartesian axis direction

Special characters

θ	[m]	Momentum thickness
δ*	[m]	Displacement thickness
φ	[deg]	Phase between actuators

ϕ	[deg]	Phase inside actuation cycle
μ	[N.m.s^{-2}]	Fluid viscosity
ω_z	[s^{-1}]	Spanwise vorticity

These flow control techniques have also been extended to include the wakes of elongated bodies having blunt-trailing edge. Clearly, such techniques would be very beneficial for the so called flatback or blunt trailing edge airfoil applications such as wind turbine blades, supercritical airfoils, etc... These airfoils have improved lift characteristics and structural integrity but because of their blunt trailing edge, they generate higher pressure drag due to the periodic low-pressure flow in their near-wake. Passive control techniques of flows over elongated bluff bodies have been reported in many investigations; Tanner [4] employed segmented, M-shaped and curved trailing edges; Grinstein et al [5] placed a splitter plate in the wake centreline; Tombazis and Bearman [6] attached a set of wavy trailing edges; Park et al. [7] attached small tabs to the trailing edge, etc... In the above studies, significant drag reduction has been achieved by suppressing the interaction between the two separating shear layers and/or affecting the vortex shedding in the vortex formation region.

Form drag reduction has also been achieved by modifying the flow momentum of the near wake of elongated bluff bodies either by trailing edge suction [8] or blowing [9,10]. Cimbala and Park [10] have shown that a proportioned injection from a slit spanning the whole width of the trailing edge of a flat plate and centrally placed achieved a "momentumless" wake with no vortex shedding. In a later study, Park and Cimbala [11] have shown that the momentumless wake dynamics strongly depended on the injection method. More recently, Henning et al. [12] and Pastoor et al. [13] employed synthetic jet actuation for active control of the wake of a plane blunt model. In their work, the authors placed two synthetic jets at the base of the model symmetrically with respect of the x- axis. The authors reported that when actuation was applied in-phase effective suppression of the vortex-shedding was obtained for actuation frequency in the range of about 0.28 to 1.15 the natural wake instability frequency. Further, operating with anti-phase forcing improved the performance of the control technique.

The objective of the current study is to investigate the physical mechanisms that achieve minimum drag and hence pressure recovery in the wake of an elongated blunt object when using an open-loop active control based on synthetic jet technology. To end this, experimental investigation of the wake flow was conducted in order to obtain a clear understanding of the control effects on the flow structures.

EXPERIMENTAL SET-UP AND MEASUREMENTS TECHNIQUES

The experiments were carried out in a low turbulence wind tunnel with a 384 x 100 mm² test section. The model was a thin flat plate having an elliptic leading (to exclude the separation-reattachment effects associated with blunt shaped leading edge on the wake dynamics) was mounted mid-height of the test section as sketched in figure 1.a. The flat plate had a length, c, of 520 mm, a thickness, h, of 12 mm, and a width, w, of 90 mm resulting in a blockage ratio of about 2%. In this work the flow velocity upstream of the model, U_∞, was 9 m/s corresponding to a Reynolds number, Re_h based on the plate's thickness h, of about 7200.

(a)

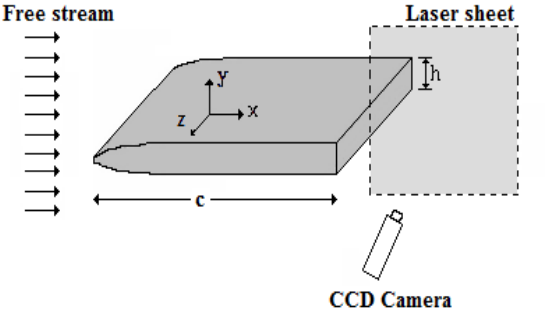

(b)

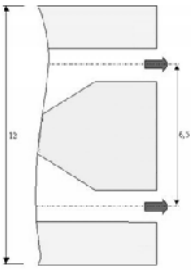

Figure 1 Experimental set-up (a) actuator positions (b).

The boundary layer developing on the surfaces of the model towards the trailing edge had a momentum thickness, θ, and displacement thickness δ* of 1.45 mm and 2.05 mm respectively. The shape factor, H, was roughly 1.41 which is typical of a turbulent boundary layer. In this study, zero-net mass flux actuation was provided using synthetic jets actuators as described in Ben chiekh et al. [14] and others. Flow control was achieved through a spanwise slot having a height, e, of 1.5 mm and a width, w_A, of 80 mm. Slots were placed at the base of the flat plate 2.5 mm from the trailing edges (peripheral slot configuration) as shown in figure 1.b. The synthetic jet momentum coefficient, Cμ, was estimated as

$$C_\mu = \frac{w_A\, e}{\pi^2\, w\, h}\,\frac{u_{A,max}^2}{U_\infty^2} \qquad (1)$$

where $u_{A,max}$ is the maximum slot exit velocity [15]. The actuation frequency f_A was selected to be 100 Hz, which is 75% the natural wake frequency in the range of values recommended by Henning et al. [12] and Pastoor et al.[13]. The actuation amplitude was adjusted to 4 V_{rms}. The governing parameters of the synthetic jet actuators at the selected frequency were $u_{A,max}$=42 m/s and Cμ=24%. The phase lag φ between the two applied excitation signals can be monitored. In the following sections, two strategies of actuation are presented: in-phase simultaneous actuation (φ=0°) and out-of-phase simultaneous actuation (φ=180°). Flow measurements were carried out using a two-dimensional PIV system (Dantec Dynamics, Ltd, Copenhagen, Denmark) including a 300 mJ double pulse Nd YAG laser (Quantel lasers) and Hi-Sense 12-bit double-frame

CCD camera (Dantec) with a resolution of 1280x1024 pixels. Free stream flow was seeded with paraffin oil smoke generated by a commercial smoke machine located at the inlet of the wind tunnel blower. Velocity vectors were computed from the particle movement observed between two successive camera exposures using Dantec FlowMap software. Adaptive cross-correlation multipass algorithm was employed with a final interrogation window size of 32x32 pixels with an overlap of 50%. The spatial resolution of the computed velocity vector field was 1.69 mm over an area of 67.89 mm x 53.96 mm. A total of 200 statistically independent samples were acquired for the average flow statistics. Assuming a sub-pixel accuracy of 0.1 pixel, the statistical error in estimating the mean velocity was about ±0.13 m/s. This corresponds to a velocity measurement accuracy of approximately 1.4%.

RESULTS AND ANALYSIS

Mean flow of the natural wake

PIV measurements were performed at downstream positions x/h up to 5.44. The cross-stream variations of the mean streamwise velocity U/U_e, where U_e is the mean streamwise velocity in the inviscid region of the flow, are plotted in Figure 2. These display the "traditional" wake-like profiles that spread laterally with increasing x/h. The length size of the separation bubble (l_b), defined by the location along the wake axis at which axial mean velocity reaches zero, is approximately 1.16h. Contour maps of the normalized, streamwise and transverse Reynolds stresses, $\overline{uu}/U_\infty^2$ and $\overline{vv}/U_\infty^2$ are shown in Fig.2b and Fig. 2c respectively. The normalized longitudinal Reynolds stress $\overline{uu}/U_\infty^2$ exhibits the characteristic distribution of wake flows having high values along the separating shear layer with two off-axis peaks of about 6% but becomes weaker outside the shear layer regions. The transverse component $\overline{vv}/U_\infty^2$ has also a symmetric distribution with large values localized within the separation bubble. Its maximum of about 15% occurred at x/h = l_b and y/h = 0 and loses its intensity farther downstream.

Effects of actuation on the wake spectra and drag

Spectra

Single hotwire measurements at x/h = 2 and y/h=1/2, were used to evaluate the spectra of the streamwise velocity fluctuations of the natural and the actuated wakes. As shown in Fig. 3, the natural wake flow was highly periodic and the coherent structures appeared as pure harmonics displaying a strong peak at the Von Karman vortex shedding frequency, f_o, of about 135 Hz. This value corresponded to a Strouhal number, St=0.18, in the range of Strouhal numbers reported in Taylor et al. [16].

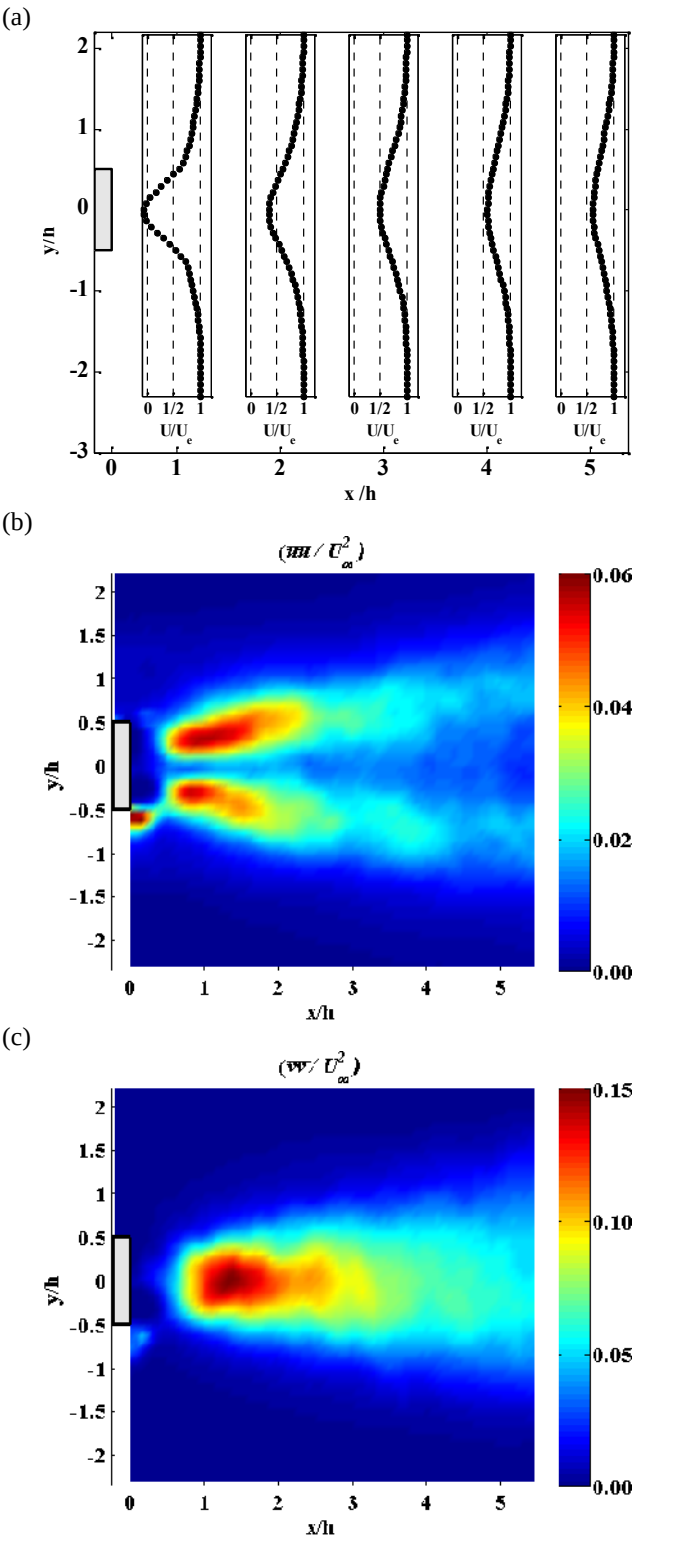

Figure 2 Natural wake features: Non-dimensional mean axial velocity U/Ue profiles (a) and distribution of the streamwise (b) and transverse (c) Reynolds stresses

When the actuation was applied, the velocity spectra in the wake showed a fundamental spectral peak at the actuating frequency, f_A (Fig. 3). A uniform 15 dB reduction in the broad band spectrum magnitude was achieved. The actuation, be it synchronous or alternate, expectedly influenced the instantaneous flow field by forming new structures which interfered with the shear layer and thus resulted in vortex shedding suppression. This vortex shedding suppression is essential for the overall drag reduction.

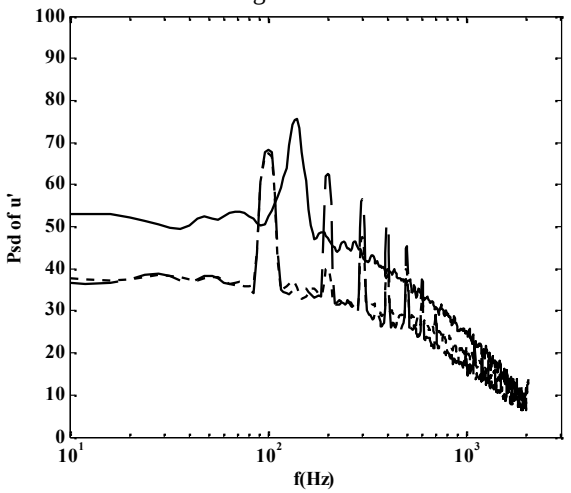

Figure 3 Spectra of the transverse velocity fluctuations measured at the location at and x/h=2 and y=h/2

. —— pure wake, ---- in-phase actuated wake, ... out-of-phase actuated wake

Drag reduction

The effect of the control strategy (synchronous and out-of-phase actuations) of the overall drag coefficient C_D, is discussed here. Estimate of the drag coefficient C_D was done using the method described in Naghib-Lahouti et al. [17]. This method, selected because of the similarity between the models used in this study and the one used in [17], depicts that:

$$C_D = 2\int_{-\infty}^{+\infty}\frac{U}{U_\infty}\left(1-\frac{U}{U_\infty}\right)\frac{dy}{h} - 2\int_{-\infty}^{+\infty}\frac{\overline{u^2}}{U_\infty^2}\frac{dy}{h} + 2\int_{-\infty}^{+\infty}\frac{\overline{v^2}}{U_\infty^2}\frac{dy}{h} + \frac{2\mu}{U_\infty^2}\int_{-\infty}^{+\infty}\left(\frac{\partial U}{\partial y}+\frac{\partial V}{\partial x}\right)\frac{dy}{h} \quad (2)$$

The first term is the drag due to the mean flow, the second and third terms correspond to the drag due to the turbulent field, and the last term is a viscous drag term that is negligible compared to the other terms. The total drag coefficient was found to be 0.93 for the natural wake, 0.13 for the synchronous actuations, and 0.08 for the alternate actuations as shown in table 1. The overall effect is that the out-of-phase actuation was more efficient in total drag reduction. This result is in agreement with the result reported in Henning and Pastoor [12]. But, each control strategy (synchronous or out-of-phase) resulted in different effect on $C_{D,mean}$ and $C_{D,turb}$, namely in the synchronous actuation case $C_{D,mean}$ = 0.18 and $C_{D,turb}$ = -0.05 and in the out-of-phase actuation $C_{D,mean}$ = -0.192 and $C_{D,turb}$ = 0.27 (see table 1). These differences are discussed in the next section.

	C_D	$C_{D,mean}$	$C_{D,turb}$
Natural wake	0.93	0.78	0.15
In-phase actuation	0.13	0.18	-0.05
Out-of-phase actuation	0.08	-0.19	0.27

Table 1 Effect of flow control on the estimated drag components

Vorticty maps

In order to explain the different contributions to the total drag under the different actuation strategy in terms of the flow structures in the actuated wake, phase-averaged velocity field synchronized with the actuation signal were performed. Figure 4 illustrates the time series evolution of the distribution of normalized spanwise vorticity within one cycle evaluated from phase-averaged velocity fields at phases ϕ=20°, 120°, 200° and 320° for the different control configurations studied. For the natural wake (Fig. 4a), the phase averaged vorticity contours, obtained using the method described in Perrin et al. [18], can be associated with the alternating vortex shedding from the two sides of the trailing edge corresponding to the well-known Karman vortex street. For in-phase actuation case (Fig. 4b), two vortex pairs of synthetic jet structures are simultaneously released at the slots exits. Actuated structures of high spanwise vorticity are shed away periodically from the synthetic jet slot. As the structures progress downstream, the two outer vortices of the synthetic jets interfered with the shear layer rollup and consequently vortex shedding is suppressed.

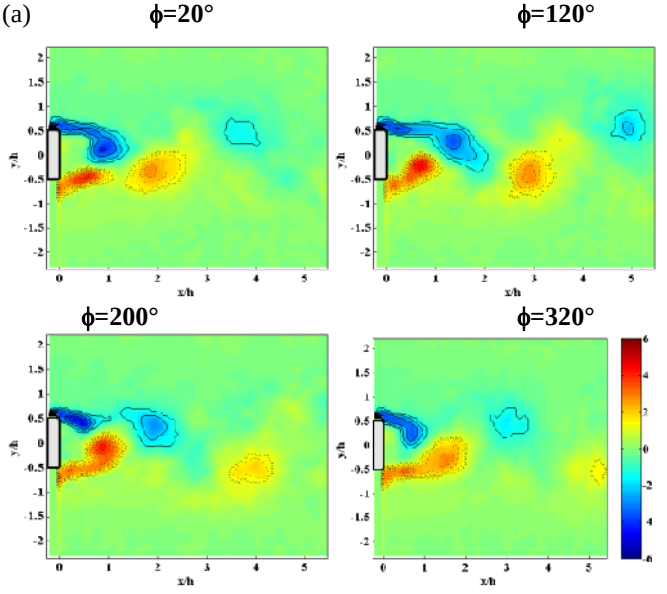

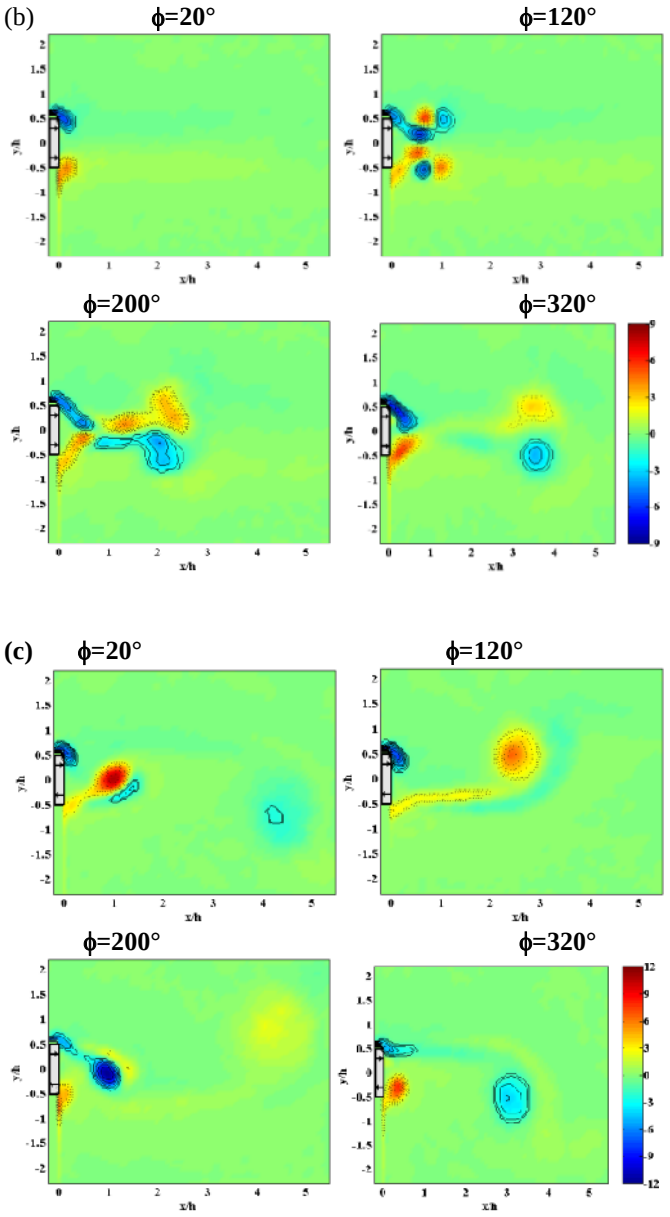

Figure 4 Distributions of normalized phase-averaged spanwise vorticity $\frac{\omega_z h}{U_\infty}$ for natural wake (a), synchronous actuated wake (b) and alternate actuated wake (c)

On the other hand, the inner vortices were unaffected by the suction phase of the actuation cycle and persisted downstream. This vortex motion enhances the momentum transfer from the high momentum, inviscid regions towards the centre of the wake. For out-of-phase dual-side actuation (Fig.4c), the effects on the wake dynamics are different in that the synthetic jet vortex pairs follow alternating paths. The decoupling of the shear layers and hence vortex shedding suppression is achieved by this synchronized alternating sequence. Indeed, the strength of the vortex pair generated by the synthetic jet is considerably magnified due to its interaction with the neighbouring shear layer. The alternate cross-flow wandering of the now much stronger vortex structures further enhances the moment transfer from the high momentum regions (the outer wake regions) towards the wake centre line.

Now that the vortex motions have been constructed for each control technique i.e. synchronous or out-of-phase actuation, the values in table 1 may be explained. Under synchronous actuation, the motion of the vortical structures remained axial with large entrainment taking place short distances downstream resulting in a nearly uniform mean velocity profile in the wake (figure 5a). This explains the considerable decrease in $C_{D,mean}$ of about 76 % reported in table 1. Furthermore, most of the turbulence production was confined to narrow regions close to trailing edge (Figures 5b & c) and was not sustained further downstream thus resulting in a decrease in the $C_{D,turb}$. In the case of the out-of-phase actuation, the vortical structures had strong cross flow motions with two structures crossing the x axis per cycle (see figure 6). This resulted in a mean velocity profile, shown in Figure 6a, resembling that of a "weak jet". This added mean momentum led to a change in the sign of $C_{D,mean}$. However as shown in figures 6b & c, the flapping nature of the vortex motion increased the turbulence in the wake with the transverse turbulent fluctuations being larger in magnitude and acting over a large region of the wake hence, the increase in $C_{D,turb}$.

CONCLUSION

The natural and actuated trailing edge wake was investigated using PIV measurements. An original arrangement of synthetic actuators has been implemented at the trailing edge of a plate model. Both synchronous and out-of-phase actuations were applied as a control strategy to reduce the overall wake drag. The actuation provided a global momentum addition Cμ=24% at an frequency equals 75% the vortex shedding frequency of the natural wake. The main conclusions of this study were (1) The mechanism with which the suppression of the natural vortex shedding is different in both control strategies; in the synchronous actuation, the outer vortices of the synthetic jets interfered with the separating shear layers rollup and in the out-of-phase actuation, the suppression due to the alternate cross-flow of the synthetic jet vortex (2) In phase (Synchronous) actuation resulted in a synchronizing both shear layers and large entrainment which led to the reduction of both components of the drag and (3) Out-of-phase jets actuation was found to be most efficient in achieving drag reduction. In this case, a considerable mean drag reduction is observed as a result the momentum addition and the "jet-like" behaviour of the mean velocity. This mean drag reduction was much larger than the drag increase due the induced transverse turbulent fluctuations.

REFERENCES

[1] Zdravkovich M. M., Flow around circular cylinder: Fundamentals, 1997, Oxford University Press, Oxford.

[2] Gad-el-Hak, M., Pollard, A., Bonnet, J.P., Flow Control: Fundamentals and Practices, 1998, New York: Springer-Verlag

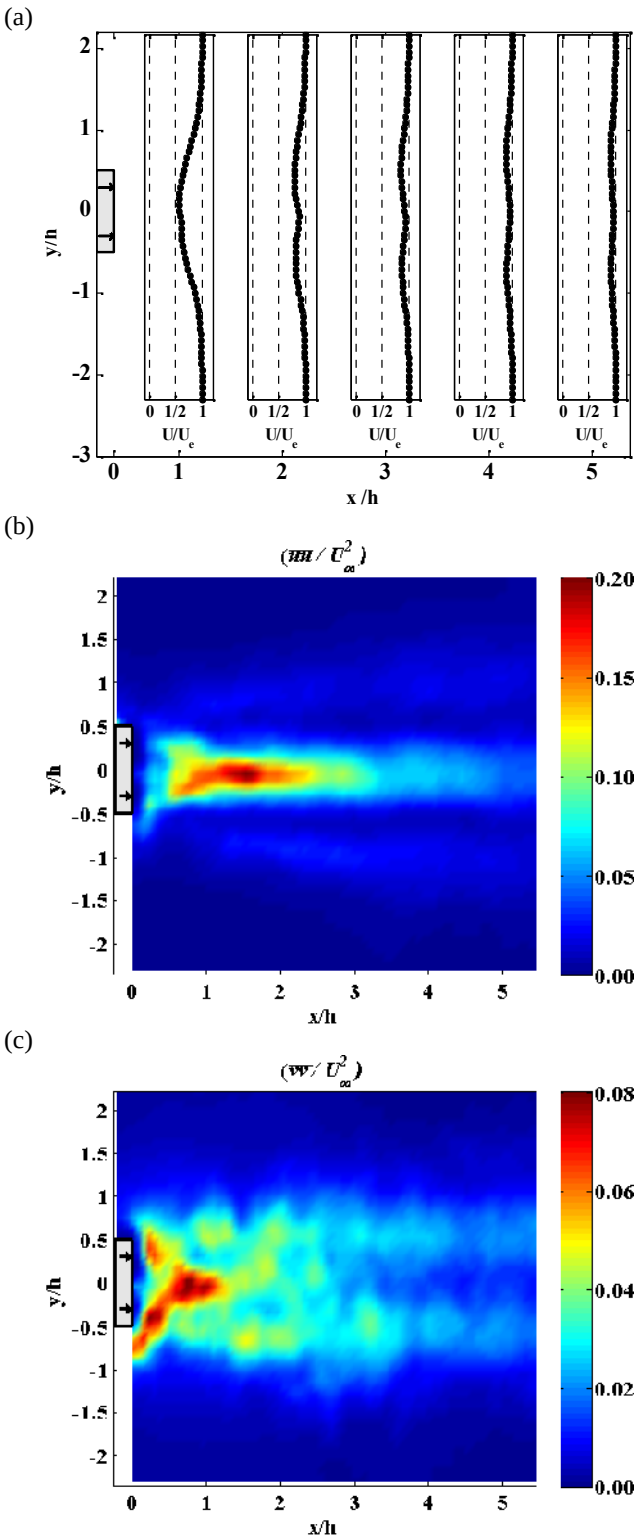

Figure 5 Non-dimensional mean axial velocity U/Ue profiles (a) and distribution of the streamwise (b) and transverse (c) Reynolds stresses for synchronous actuated wake

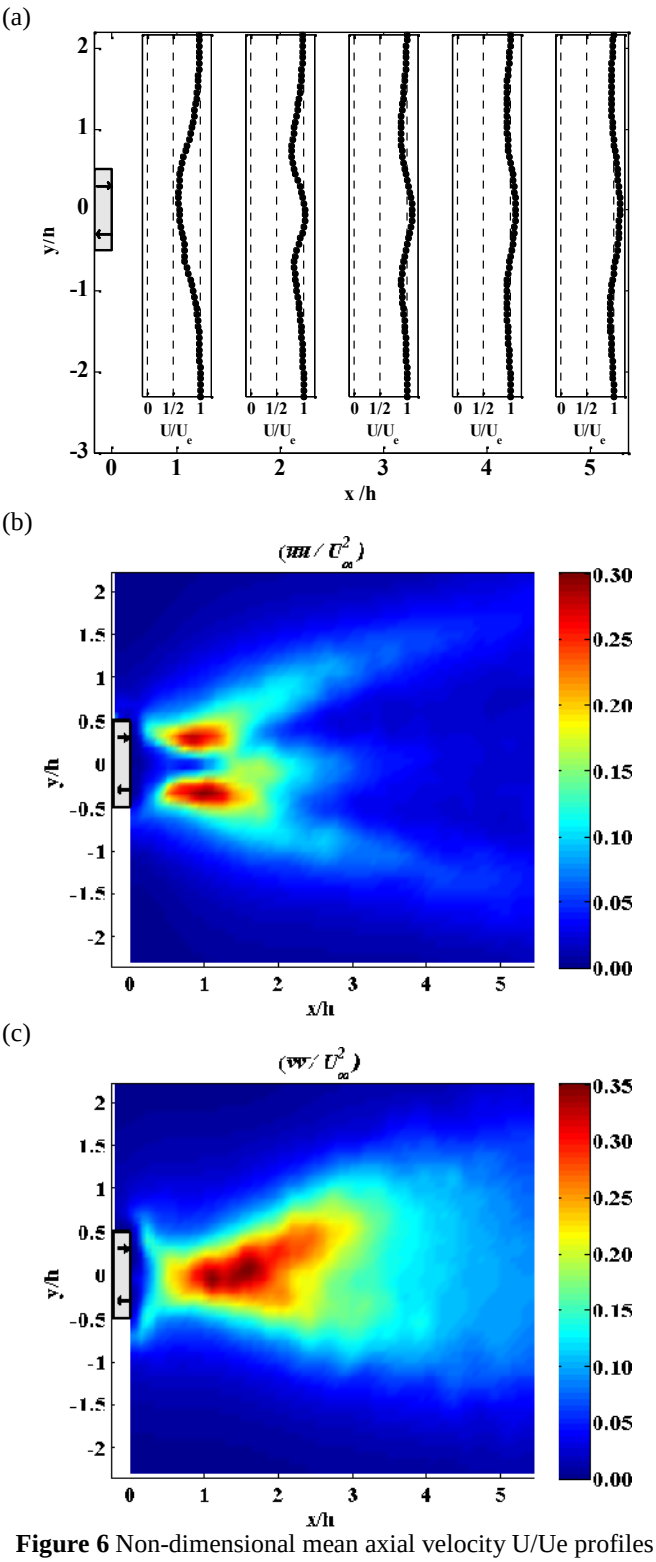

Figure 6 Non-dimensional mean axial velocity U/Ue profiles (a) and distribution of the streamwise (b) and transverse (c) Reynolds stresses for alternate actuated wake

[3] Choi, H., Jeon, W.P., Kim, J., Control of flow over bluff body, *Ann. Rev. Fluid Mech.*, vol 40, 2008, pp. 113-139
[4] Tanner, M., New Investigation for Reducing the Base Drag of Wings with a Blunt Trailing Edge. *Aerodynamic Drag*, AGARD-CP-124, 1973, 12-1–12-9
[5] Grinstein, F. F., Boris, J. P., Griffin, O. M., Passive pressure-drag control in a plane wake, *AIAA Journal*, Vol. 29, 1991, pp.1436–1442
[6] Tombazis, N. and Bearman, P. W., A Study of Three-Dimensional Aspects of Vortex Shedding from a Bluff Body with a Mild Geometric Disturbance, *Journal of Fluid Mechanics*, Vol. 330, 1997, pp. 85-112
[7] Park, H, Li, D., Jeon, W. P., Hahn, S., Kim, J., Kim, J., Choi, J, Choi, H., Drag reduction in flow over a two-dimensional bluff body with a blunt trailing edge using a new passive device, *Journal of Fluid Mechanics*, Vol. 563, 2006, pp. 389–414
[8] Sharma, S. D., Sahoo R. K., Control of the periodic wake behind a plane blunt base, *In fluid mechanics and its applications, 53, Proceedings of IUTAM Symposium on Mechanics of Passive and Active Flow Control* (eds)GEAMeier and PRViswanath (Dordrecht/Boston/London: Kluwer Academic), 1998, pp. 267–272.
[9] Wu, Y., Zhu, X., Du, Z., Experimental investigation on the momentumless wake using trailing edge blowing, *IMechE Vol. 222 Part C: J. Mechanical Engineering Science*, 2008, pp. 1478-1486
[10] Cimbala, J.M. and Park, W.J., An experimental investigation of the turbulent structure in two-dimensional momentumless wake, *Journal of Fluid Mechanics*, Vol. 213, 1990, pp. 479–509
[11] Park, W.J., and Cimbala, J.M., The effects of jet injection geometry on two-dimensional momentumless wakes. *Journal of Fluid Mechanics*, Vol. 224, 1991, pp. 29–47
[12] Henning, L., Pastoor, M., King, R., Noack, B., Tadmor, G., Feedback control applied to the bluff body wake. In R. King, ed., *Active Flow Control*, Vol. 95 of Notes on Numerical Fluid Mechanics and Multidisciplinary Design, 2007, Springer
[13] Pastoor, M., Henning, L., Noack, B.R., King, R., Tadmor, G., Feedback shear layer control for bluff body drag reduction, *Journal of Fluid Mechanics*, Vol. 608, 2008, pp. 161-196
[14] Ben Chiekh, M., Béra, J.C., Sunyach, M., Synthetic jet control of a confined flow through a wide-angle diffuser: flow control mechanisms, *Journal of Turbulence*, Vol. 4,No. 32, 2003
[15] Holman, R., Utturkar, Y., Mittal, R., Smith B., Cattafesta L., Formation criteria for synthetic jets, AIAA Journal, Vol. 43, 2005, pp. 2110-2116
[16] Taylor, Z.J., Palombi, E., Gurka, R., Kopp G.A., Features of the turbulent flow around symmetric elongated bluff bodies, *Journal of Fluids and Structures*, Vol. 27, 2011, pp. 250-265
[17] Naghib-Lahouti, A., Doddipatla, L. S., Hangan H., Secondary wake instabilities of a blunt trailing edge profiled body as a basis for flow control, *Experiments in Fluids*, 2012, pp.
[18] Perrin, R., Braza M., Cid, E., Cazin, S., Barthet A., Sevrain A., Mockett C., Thiele F., Obtaining phase averaged turbulence properties in the near wake of a circular cylinder at high Reynolds number using POD, *Experiments in Fluids*, Vol. 43, 2007, pp. 341-355.